J|A|C|S
ARTICLES
Published on Web 12/06/2006

Chiral Self-Recognition: Direct Spectroscopic Detection of the Homochiral and Heterochiral Dimers of Propylene Oxide in the Gas Phase

Zheng Su, Nicole Borho, and Yunjie Xu*

Contribution from the Department of Chemistry, University of Alberta Edmonton, Alberta, Canada, T6G 2G2

Received August 23, 2006; E-mail: yunjie.xu@ualberta.ca

Abstract: In this report, we describe rotational spectroscopic and high-level ab initio studies of the 1:1 chiral molecular adduct of propylene oxide dimer. The complexes are bound by weak secondary hydrogen bonds, that is, the $O_{epoxy}\cdots H-C$ noncovalent interactions. Six homochiral and six heterochiral conformers were predicted to be the most stable configurations where each monomer acts as a proton acceptor and a donor simultaneously, forming two six- or five-membered intermolecular hydrogen-bonded rings. Rotational spectra of six, that is, three homochiral and heterochiral conformer pairs, out of the eight conformers that were predicted to have sufficiently large permanent electric dipole moments were measured and analyzed. The relative conformational stability order and the signs of the chiral recognition energies of the six conformers were determined experimentally and were compared to the ab initio computational results. The experimental observations and the ab initio calculations suggest that the concerted effort of these weak secondary hydrogen bonds can successfully lock the subunits in a particular orientation and that the overall binding strength is comparable to a classic hydrogen bond.

Introduction

Chiral recognition is the ability of a chiral molecule to distinguish between the two enantiomeric forms of another chiral molecule.[1] One important question is how the intermolecular forces act in a concerted way to enable the substantial enantioselectivity in many natural processes. Enantiomeric discrimination is also the basis of chiral chromatography,[2] asymmetric synthesis, and nuclear magnetic resonance (NMR) analysis of enantiomeric purity.[3] Although these techniques are evidently consequence of enantioselectivity on the basis of different interaction energies of the *RR* and *RS* diastereomeric pairs,[4] there is very little quantitative experimental information on the nature of these interactions and their contributions to chiral discrimination on the molecular level. Very recently, Soloshonok reported that nonracemic mixtures of chiral molecules containing perfluoromethyl groups exhibit remarkable amplification of the self-disproportionation[5] and that putting such mixtures through an achiral-Si gel column can produce an *ee* as high as 99% depending on the effluents used. This underscores the importance in understanding the interactions among chiral molecules and between chiral molecules and solvent molecules.

Spectroscopic studies of chiral molecular complexes formed in a supersonic expansion were first reported by the groups of Zehnacker-Rentien and Giardini-Guidoni in an effort to provide quantitative evidence of enantiomeric selection. These groups have studied complexes composed of a chiral aromatic derivative and a chiral alcohol using laser-induced fluorescence,[6] hole-burning,[7] and resonance-enhanced multiphoton ionization spectroscopy.[9] More recently, Suhm and co-workers used ragout-jet Fourier transform (FT) infrared (IR) spectroscopy to probe vibrational band structures of many chiral and transient chiral molecular complexes, such as glycidol dimer,[10] binary, ternary,[11] and even larger aggregates of lactates,[12] ethanol dimer,[13] and fluoroethanol dimer.[14] The first high resolution spectroscopic study of a chiral molecular complex, that is, butan-2-ol dimer,[15] was reported by Howard and co-workers, where one heterochiral dimer was assigned. Subsequently, the same group published a rotational study of ethanol dimer, focusing on the transient chirality of the molecular system.[16] High resolution spectroscopy is sensitive to even the subtlest differences in the structures.

(1) Cantor, C. R.; Schimmel, P. R. *Biophysical Chemistry* W. H. Freeman: San Francisco, CA, 1980.
(2) Pirkle, W. H.; Pochapsky, T. G. *Chem. Rev.* **1989**, *89*, 347−362.
(3) Parker, D. *Chem. Rev.* **1991**, *91*, 1441−1457.
(4) Buckingham, A. D.; Fischer, P. *Chem. Phys.* **2006**, *324*, 111−126.
(5) Soloshonok, V. A. *Angew. Chem., Int. Ed.* **2006**, *45*, 165−168.
(6) Alrabaa, A.; Le Barbu, K.; Lahmani, F.; Zehnacker-Rentien, A. *J. Phys. Chem. A* **1997**, *101*, 3273−3278.
(7) Le Barbu, K.; Brenner, V.; Millié, Ph.; Lahmani, F.; Zehnacker-Rentien, A. *J. Phys. Chem. A* **1998**, *102*, 128−137.
(8) Piccirillo, S.; Bosman, C.; Toja, D.; Giardini-Guidoni, A.; Pierini, M.; Troiani, A.; Speranza, M. *Angew. Chem., Int. Ed. Engl.* **1995**, *36*, 1729−1731.
(9) Latinia, A.; Toja, D.; Giardini-Guidoni, A.; Piccirillo, S.; Speranza, M. *Angew. Chem., Int. Ed.* **1999**, *38*, 815−817.
(10) Borho, N.; Haber, Th.; Suhm, M. A. *Phys. Chem. Chem. Phys.* **2001**, *3*, 1945−1948. Borho, N.; Suhm, M. A. *Phys. Chem. Chem. Phys.* **2002**, *4*, 2721−2732.
(11) Borho, N.; Suhm, M. A. *Org. Biomol. Chem.* **2003**, *1*, 4351−4358.
(12) Adler, T. B.; Borho, N.; Reiher, M.; Suhm, M. A. *Angew. Chem.* **2006**, *45*, 3440−3445.
(13) Emmeluth, C.; Dyczmons, V.; Kinzel, T.; Botschwina, P.; Suhm, M. A.; Yáñez, M. *Phys. Chem. Chem. Phys.* **2005**, *7*, 991−997.
(14) Scharge, T.; Emmeluth, C.; Häber, T.; Suhm, M. A. *J. Mol. Struct.* **2006**, *786*, 86−95.
(15) King, A. K.; Howard, B. J. *Chem. Phys. Lett.* **2001**, *348*, 343−349.

10.1021/ja066128j CCC: $33.50

Also, the rotationally resolved spectra can be used to obtain accurate structural information of different conformers that is difficult to extract from the low-resolution electronic or FTIR measurements mentioned above. The very limited high resolution spectroscopic data of chiral molecular complexes highlight the fact that to achieve unambiguous assignment of rotationally resolved spectra of chiral molecular systems with many potential conformers is a daunting task. To aid the spectroscopic studies, a small number of high-level quantum chemistry studies have been dedicated to the investigations of chiral discrimination effects of suitable small chiral molecules. Portmann et al. investigated chiral recognition in the complexes of hydrogen peroxide (H_2O_2) with propylene oxide (PO) and its derivatives.[17] Our group carried out detailed studies on the hydrogen (H)-bonded molecular complex between propylene imine and H_2O_2.[18] Alkorta and Elguero studied a series of β-aminoalcohols and H-bonded complexes consisting of compounds with axial chirality.[19,20]

In this article, we report detailed rotational spectroscopic and high-level ab initio studies of chiral self-recognition in PO dimer in the gas phase. PO is a simple cyclic ether chiral molecule and is chemically stable. It has one stereogenic center: the carbon atom bonded with the methyl group. Although the structure of PO monomer was well determined by microwave (MW) spectroscopy a long time ago,[21−23] the rotational investigations of the rare gas (RG) atom (RG = Ne,[24,25] Ar,[26] Kr[27]) and PO adducts were actually the very first studies of the PO containing van der Waals complexes. Recently, we investigated the H-bonded PO−water complex,[28] where the subtle yet decisive stabilizing contribution of the methyl group through a secondary H-bond was observed. In the following sections, we describe the first high resolution spectroscopic assignment of six homo- and heterochiral conformers of PO dimer. We focus our attention on the weak secondary H-bonds, that is, the $O_{epoxy}\cdot\cdot\cdot H-C$ noncovalent interactions, and their roles in the chiral self-discrimination process in PO dimer.

Ab Initio Calculations

Even for a simple chiral molecular system such as PO, the number of possible binary conformers is surprisingly large. On the basis of chemical intuition, more than 20 preliminary structures were proposed originally. These structures can be divided into two groups, differing in the number of the secondary H-bonds utilized in each conformer. The first group emphasizes that each PO monomer accepts two protons from and donates two protons to the other monomer simultaneously. The two PO subunits are connected through these four secondary H-bonds, forming two six- or five-membered intermolecular H-bonded rings. Statistically, this group consists of six homochiral and six heterochiral conformers. In the second group, each monomer can only act as either proton acceptor or donor, that is, only two intermolecular H-bonds are formed in each conformer.

Table 1. Calculated Raw and Counterpoise-Corrected Dissociation Energies (in kJ/mol), Rotational Constants (in MHz), and Electric Dipole Moment Components (in Debye) of the Homochiral and Heterochiral Conformers of PO Dimer at the MP2/6-311++G(d,p) Level of Theory

	D_e	$D_e + CP$	A	B	C	$\lvert\mu_a\rvert$	$\lvert\mu_b\rvert$	$\lvert\mu_c\rvert$
*RR*1	−23.55	−15.31	3013	1131	1007	0.01	0.04	0.00
*RS*1	−22.95	−14.98	3168	1116	939	0.01	0.00	0.01
*RR*2	−22.98	−14.97	3171	1111	932	0.52	0.54	0.03
*RS*2	−22.92	−14.91	3179	1048	1013	0.58	0.35	0.23
*RR*3	−22.42	−14.36	3363	1020	958	0.00	0.00	0.59
*RS*3	−21.97	−14.05	3290	1095	887	0.00	0.00	0.00
*RR*4	−22.84	−14.79	3838	970	874	0.18	0.26	0.06
*RS*4	−23.21	−14.92	3454	1025	904	0.23	0.22	0.18
*RR*5	−22.34	−14.22	3707	967	893	0.78	0.20	0.42
*RS*5	−22.15	−14.22	3833	948	857	0.67	0.77	0.03
*RR*6	−22.60	−14.46	3934	912	821	0.00	0.43	0.00
*RS*6	−22.55	−14.44	4866	851	801	0.00	0.00	0.00

To provide valuable clues for the spectroscopic study,[28,29] we carried out a series of geometry optimizations for the possible homo- and heterochiral dimers using the Gaussian03 software package.[30] Second-order Møller-Plesset perturbation theory (MP2)[31] with the basis set 6-311++G(d,p)[32] was employed for full geometry optimizations. The conformers in the second group were predicted to have about half of the dissociation energies compared to those of the first group and were thus being excluded from further experimental searches. The 12 proposed structures of the first group were all found to be local minima. The raw and counterpoise-corrected[33] dissociation energies, rotational constants, and electric dipole moment components for the above 12 optimized structures calculated with MP2/6-311++G(d,p) are summarized in Table 1. It was noticed that the differences in the rotational constants of some of these conformers are very small. Therefore, to be certain about the proposed configurations, we also carried out additional geometry optimization calculations using three more basis sets: 6-311++G-(2d, 2p), aug-cc-pVDZ,[34] and a mixed basis set, that is, aug-cc-pVDZ for the heavy atoms C and O and 6-311++G(d,p) for the H atoms, respectively. The results for the 12 optimized structures calculated with the three additional basis sets are shown in Table S1, available as Supporting Information. In general, the values predicted by all four basis sets agree with each other, confirming the distinct identity of each configuration. For the few conformers with similar rotational constants, their dipole moment components differ enough to show distinguishable spectral pattern. For simplicity, we will use the result from MP2/6-311++G(d,p) in the remainder of the paper and refer to the results by the other three basis sets only when needed.

(16) Hearn, J. P. I.; Cobley, R. V.; Howard, B. J. *J. Chem. Phys.* **2005**, *123*, 134324/1−7.
(17) Portmann, S.; Inauen, A.; Lüthi, H. P.; Leutwyler, S. *J. Chem. Phys.* **2000**, *113*, 9577−9585.
(18) Su, Z.; Xu, Y. *Phys. Chem. Chem. Phys.* **2005**, *7*, 2554−2560.
(19) Alkorta, I.; Elguero, J. *J. Am. Chem. Soc.* **2002**, *124*, 1488−1493.
(20) Alkorta, I.; Elguero, J. *J. Chem. Phys.* **2002**, *117*, 6463−6468.
(21) Swalen, J. D.; Herschbach, D. R. *J. Chem. Phys.* **1957**, *27*, 100−108.
(22) Herschbach, D. R.; Swalen, J. D. *J. Chem. Phys.* **1958**, *29*, 761−776.
(23) Imachi, M.; Kuczkowski, R. L. *J. Mol. Struct.* **1982**, *96*, 55−60.
(24) Blanco, S.; Maris, A.; Melandri, S.; Caminati, W. *Mol. Phys.* **2002**, *100*, 3245−3249.
(25) Su, Z.; Xu, Y. *J. Mol. Spectrosc.* **2005**, *232*, 112−114.
(26) Blanco, S.; Maris, A.; Millemaggi, A.; Caminati, W. *J. Mol. Struct.* **2001**, *612*, 309−313.
(27) Blanco, S.; Melandri, S.; Maris, A.; Caminati, W.; Velino, B.; Kisiel, Z. *Phys. Chem. Chem. Phys.* **2003**, *5*, 1359−1364.
(28) Su. Z.; Wen, Q.; Xu, Y. *J. Am. Chem. Soc.* **2006**, *128*, 6755−6760.
(29) Su, Z.; Tam, W. S.; Xu, Y. *J. Chem. Phys.* **2006**, *124*, 024311/1−9.
(30) Pople, J. A. et al. *Gaussian 03*, Revision B.01; Gaussian, Inc.: Pittsburgh, PA, 2003.
(31) Binkley, J. S.; Pople, J. A. *Int. Quantum Chem.* **1975**, *9*, 229−236.
(32) Krishman, R.; Binkley, J. S.; Seeger, R.; Pople, J. A. *J. Chem. Phys.* **1980**, *72*, 650−654.
(33) Boys, S. F.; Bernardi, F. *Mol. Phys.* **1970**, *10*, 553−566.
(34) Woon, D. E.; Dunning, T. H., Jr. *J. Chem. Phys.* **1993**, *98*, 1358−1371.

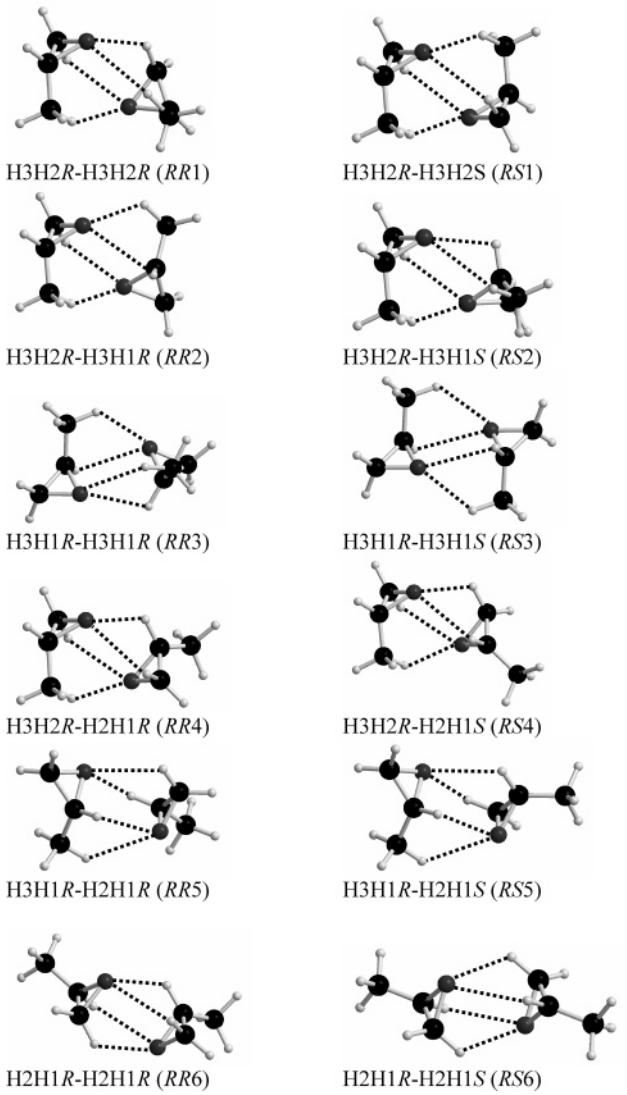

Figure 1. Optimized geometries at the MP2/6-311++G(d,p) level of theory of six homochiral (*RR*) and six heterochiral (*RS*) conformers of PO dimer. The corresponding notation for each conformer takes the form of HxHy*R*-Hx′Hy′*R*/*S* (see text for details).

The MP2/6-311++G(d,p) optimized structures of the 12 conformers of PO dimer are shown in Figure 1. We proposed a unique notation for the conformational structures under consideration. It is of the form H*x*H*y*R-H*x*′H*y*′*R* or *S* where *R* or *S* specifies the chirality of the monomer subunit. The *RR* or *SS* combination indicates homochiral dimer, while the *RS* or *SR* label means heterochiral dimer. Since the *SS* and *RR* of a particular configuration give the same rotational spectrum and the same is true for the *RS* and *SR* pair, *R* notation is always used for the first subunit for simplicity. The letters *x*, *y*, and *x*′, *y*′ take the integer values of 1, 2, or 3, indicating that the corresponding hydrogen atoms are from the CH, CH_2, or CH_3 sites, respectively. For easy bookkeeping, the integers are kept in descending order in each monomer subunit. Thus, in the nomenclature described here, H3H2*R*-H2H1*S* represents a heterochiral dimer with four intermolecular H-bonds where CH_3 and CH_2 of *R*-PO each contributes one H atom to the O atom of *S*-PO and the other two H atoms from CH_2 and CH of *S*-PO point towards the O atom of *R*-PO. The notation introduced here provides important information about the binding sites in each conformer and is given in Figure 1 for all 12 configurations. We will use this notation later in the discussion of stability order and chiral self-recognition where specific binding sites are relevant. To make our presentation more concise and easier for the readers, we further simplify the labeling for the six homochiral conformers as *RR*1−*RR*6 and the corresponding heterochiral conformers as *RS*1−*RS*6 (see Figure 1).

Experimental Section

A pulsed molecular beam FTMW spectrometer,[35] operated in the frequency region between 4 and 26 GHz, was used in this study. For the investigations of the homochiral species, a gas mixture of less than 1.0% enantiomeric *R*-PO (≥99.0%, Aldrich) in 6.5 bar helium (Praxair) at room temperature was expanded through a General Valve (Series 9, 0.8 mm). A racemic mixture of PO (99+%, Aldrich) was used for the spectral searches and measurements of the heterochiral dimers and for the intensity investigation of all homo- and heterochiral diastereomers. The full line width at half-height of a well-resolved line is about 18 kHz and the uncertainty of the frequency measurements is ∼2 kHz. The estimated effective rotational temperature in the helium expansion is 2.5 K.

Rotational Spectra

The initial spectral scan was carried out in the 4−7 GHz range for the low *J* transitions of *RR* conformers. A very rich spectrum was obtained. To be sure about the identity of the line carriers, test measurements were conducted with neon as carrier gas instead of helium and with racemic PO instead of enantiopure PO. In the previous jet-cooled rotational spectroscopic studies of van der Waals complexes, for example, dimethyl ether dimer,[36] only the lowest energy conformer was detected. However, the spectral search for *RR*1, which was predicted to be the most stable conformer of all, may be difficult here because of its small electric dipole moments. On the other hand, the FTMW spectroscopy was successfully utilized for the studies of mixed rare gas clusters whose dipole moments were estimated to be in the same order of magnitude or smaller than that of *RR*1 conformer.[37] As it turned out, none of the observed lines could be assigned satisfactorily to this lowest energy configuration without dramatic changes in the shape of the conformer. We therefore moved on to other homochiral configurations. Indeed, nine previously observed lines could be assigned to the *a*-type transitions of the second lowest energy homochiral configuration, *RR*2. The *b*-type and the much weaker *c*-type transitions were then predicted on the basis of the initial fit and were successfully located. The *a*- and *b*-type transitions require similar optimized MW excitation pulse width, while the optimized MW pulse widths for the *c*-type transitions are much longer. This observation is in accord with the ratio of the dipole moment components predicted by MP2/6-311++G(d,p) calculations. The experimental magnitudes of the dipole moment components, estimated by comparing the optimized pulsed widths to that of carbonyl sulphide (OCS) with a known dipole moment of 0.7149 D,[38] are also consistent with the prediction. The assignment of the observed lines to this particular conformer is therefore not only verified by the similarity of the observed and calculated rotational constants but is also further reinforced by the good agreement between the experimentally estimated and theoretically predicted electric dipole moment properties.

(35) Xu, Y.; Jäger, W. *J. Chem. Phys.* **1997**, *106*, 7968−7980.
(36) Tatamitani, Y.; Liu, B.; Shimada, J.; Ogata, T.; Ottaviani, P.; Maris, A.; Caminati, W.; Alonso, J. L. *J. Am. Chem. Soc.* **2002**, *124*, 2739−2743.
(37) Xu, Y.; Jäger, W. *J. Chem. Phys.* **1997**, *107*, 4788−4796.
(38) Dijkerman, H. A.; Ruitenberg, G. *Chem. Phys. Lett.* **1969**, *3*, 172−174.

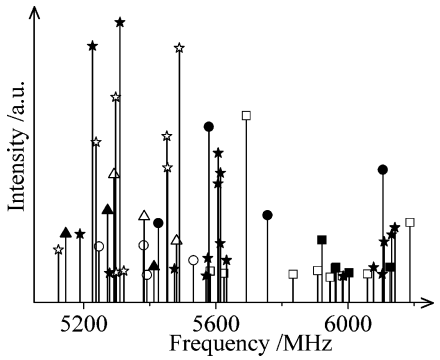

Figure 2. Observed rotational transitions with the enantiomeric *R*-PO and racemic PO samples. The transitions are assigned to *RR*2 (□), *RR*4 (○), *RR*5 (△), *RS*2 (■), *RS*4 (●), and *RS*5 (▲). ☆ represents unassigned lines in the enantiopure sample; ★ indicates unassigned lines only in the racemic sample but not in the enantiopure one.

In addition to *RR*2 conformer, 10 *a*-type transitions of *RR*5 were found. The magnitude of the *a*-dipole moment component is estimated to be about 1.5 times larger than that of *RR*2, in general agreement with the prediction. The searches for the *a*-type transitions of *RR*4 were more difficult and the corresponding transitions were detected only after we lengthened the MW pulse width significantly. That ties in well with the fact that the predicted *a*-dipole moment component is several times smaller than that of *RR*2 or *RR*5. In total, seven lines were assigned to the *a*-type transition with J up to 4 and K_a up to 2. Searches for the *b*- and *c*-type transitions of *RR*4 and *RR*5 were attempted, but no concrete assignments were achieved. Although a few candidates were located for *RR*3 and *RR*6 in the spectral searches, no satisfactory assignment could be obtained since these two conformers have only *c*- or *b*-type transitions whose patterns are much more difficult to recognize than the *a*-type transitions.

The searches and assignments for the heterochiral PO dimers followed the procedure described above. The three configurations, that is, *RS*2, *RS*4, and *RS*5, predicted to have substantial electric dipole moment values, were identified successfully. The experimentally estimated magnitudes of the *a*-, *b*-, and *c*-dipole moments are again in reasonable agreement with the MP2/6-311++G(d,p) predictions. In total, 42 lines were measured for the heterochiral PO dimers: 17 for *RS*2, 11 for *RS*4, and 14 for *RS*5. These transitions are not present using the enantiopure PO sample. The remaining three *RS* conformers have basically zero electric dipole moments, and no spectral searches were attempted for them. Figure 2 shows all the transitions detected in both the enantiopure and racemic PO samples in a 1 GHz frequency span, plotted with the observed relative intensity ratio. Several unassigned transitions are also shown. Although experimental evidence indicates that the carriers of these unassigned transitions are most likely due to the binary or larger PO clusters, their exact identities are not yet determined.

The measured rotational transition frequencies of the six PO dimers are summarized in Table S1, available as Supporting Information. They were fitted to a Watson's S-reduction semirigid rotor Hamiltonian in its I^r-representation.[39] The resulting spectroscopic constants are listed in Tables 2 and 3 for the homo- and heterochiral diastereomers, respectively. The

(39) Watson, J. K. G. In *Vibrational Spectra and Structure: A series of Advances;* Durig, J. R., Ed.; Elsevier: New York, 1977; Vol. 6, p 1.

Table 2. Experimental Rotational and Centrifugal Distortion Constants of the Three Homochiral Conformers of PO Dimer

	*RR*2	*RR*4	*RR*5
A/MHz	3157.9758 (6)[a]	3799.5 (4)	3728.3 (3)
B/MHz	1073.4876 (1)	946.0501 (7)	929.3788 (4)
C/MHz	908.3481 (1)	850.8587 (6)	866.3289 (4)
D_J/kHz	0.678 (2)	0.60 (1)	0.577 (6)
D_{JK}/kHz	3.020 (8)	0.1 (2)	0.6 (3)
D_K/kHz	−2.7 (1)	0.0[b]	0.0[b]
d_1/kHz	−0.127 (2)	−0.11 (1)	−0.047 (4)
d_2/kHz	−0.029 (1)	0.0[b]	0.006 (3)
N[c]	36	7	10
σ/kHz[d]	4.9	0.4	1.1

[a] Standard errors in parentheses are expressed in units of the last digits. [b] Fixed at 0.0 in the fit. [c] Number of transitions in the fit. [d] rms deviation of the fit.

Table 3. Experimental Rotational and Centrifugal Distortion Constants of the Three Heterochiral Conformers of PO Dimer

	*RS*2	*RS*4	*RS*5
A/MHz	3186.5835 (9)[a]	3473.684 (2)	3808.5 (3)
B/MHz	1007.4002 (2)	987.2129 (6)	924.5426 (3)
C/MHz	980.0498 (2)	877.1365 (5)	835.6008 (4)
D_J/kHz	0.711 (3)	0.697 (9)	0.46 (2)
D_{JK}/kHz	−0.8(2)	0.4 (1)	0.9 (3)
D_K/kHz	2.33 (3)	7.7 (8)	0.2 (3)
d_1/kHz	−0.047 (2)	−0.05 (2)	−0.051 (4)
d_2/kHz	−0.004 (3)	1.2 (4)	−0.018 (9)
N[b]	17	11	14
σ/kHz[c]	3.7	4.4	0.5

[a] Standard errors in parentheses are expressed in units of the last digits. [b] Number of transitions in the fit. [c] rms deviation of the fit.

standard deviations of the spectroscopic fits are a few kHz, in good agreement with the experimental uncertainty.

Conformational Geometries

With the MP2/6-311++G(d,p) calculations, the largest deviation from the experimental rotational constants is 41 MHz, while that of MP2/6-311++G(2d,2p), MP2/aug-cc-pVDZ, and the mixed basis set, that is, aug-cc-pVDZ/6-311++G(d,p), is 58, 101, and 67 MHz, respectively. Here, the MP2/6-311++G(d,p) calculation provides the best agreement. Similar conclusions were made in our previous rotational spectroscopic study of the PO−water adduct[28] and the infrared spectroscopic study of the cyclopropane−CO_2 adduct.[29] The rotational constants alone may not provide enough discrimination for the unambiguous assignment of a particular conformer since some conformers have very similar predicted rotational constants (see Table 1). In these cases, the information on the electric dipole moment components and the experimental distinction whether a dimer is homo- or heterochiral serve as additional identification criteria. The small differences between the observed and the MP2/6-311++G(d,p) rotational constants as well as the good agreements for the electric dipole moment components lead us to the conclusion that the actual structures of the measured dimer species are very close to the MP2/6-311++G(d,p) optimized geometries. The most important intermolecular structural parameters are defined in Figure 3 using *RR*2 as an example. Here, d is the H-bonding distance $O_{expoxy}\cdots H$; θ is the H-bonding angle, $\angle O_{expoxy}\cdots H-C$; and τ is $\angle H\cdots O_{expoxy}\cdots H$. The subscripts 1−4 illustrated in Figure 3 define the appearance of each set of the structural parameters from top to bottom in every configuration as shown in Figure 1. The ab initio values of these structural parameters for the six observed conformers are listed in Table 4. The H-bond length ranges from 2.46 to 2.85 Å,

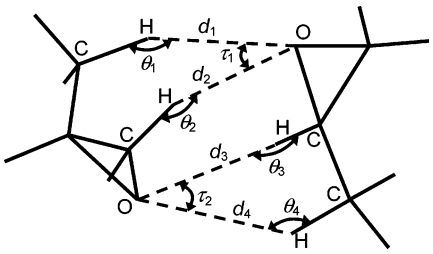

Figure 3. Definition of the most important H-bond structural parameters for PO dimer.

Table 4. Secondary Hydrogen Bond Structural Parameters of the Six Experimentally Observed Conformers of PO Dimer at the MP2/6-311++G(d,p) Calculations[a]

	*RR*2	*RS*2	*RR*4	*RS*4	*RR*5	*RS*5
d_1/Å	2.502	2.770	2.586	2.617	2.613	2.568
d_2/Å	2.454	2.704	2.692	2.652	2.523	2.562
d_3/Å	2.875	2.463	2.542	2.534	2.811	2.838
d_4/Å	2.577	2.507	2.572	2.576	2.625	2.618
θ_1/deg	148.8	100.3	120.1	117.3	114.8	117.8
θ_2/deg	130.8	121.7	114.9	117.7	119.4	116.5
θ_3/deg	95.6	130.8	125.9	125.9	94.9	94.1
θ_4/deg	125.3	148.6	145.3	145.1	121.9	122.5
τ_1/deg	60.1	55.2	55.8	55.9	57.6	57.7
τ_2/deg	55.2	60.0	57.6	57.8	55.5	55.3

[a] The structural parameters are defined in Figure 3.

which falls in the general range expected for this type of secondary H-bonds. The H-bond angle varies from 95 to 149 degrees, while the magnitude of τ changes from 55 to 60 degrees for the homo- and heterochiral pairs. The relative difference between the experimental and calculated *A* rotational constant is the smallest among the three rotational constants and can be either positive or negative. On the other hand, the ab initio calculation consistently overestimates the magnitude of *B* and *C* constants by 1−4% at the MP2/6-311++G(d,p) level. This implies that the actual structures of the six observed conformers are slightly more compact than predicted.

Secondary H-Bonds, Conformational Stability, and Chiral Diastaltic Energies

The counterpoise-corrected dissociation energies by MP2/6-311++G(d,p) of all the 12 conformers involving four intermolecular secondary H-bonds are about −15 kJ/mol, surprisingly close to those of the strongly H-bonded PO−H_2O conformers at −21 kJ/mol. Furthermore, the detection of six distinct conformers of this molecular adduct bound only by weak secondary H-bonds is somewhat unexpected since one may expect it to be a floppy system with a relatively flat minimum and large amplitude motions. Our experiment shows that even though the dissociation energy of one secondary H-bond is much smaller than a classic H-bond, the sum of all four possible secondary H-bonds could have an effect as large as one strong H-bond. The direct detection of six distinct conformers implies that although these secondary H-bonds are relatively weak in binding strength, they can play a significant role in locking the binding subunits in a specific position. These observations suggest that the secondary H-bond interactions may play an important role in many biological processes, a subject of intense current interest,[40−42] since secondary H-bonds are very common in the much larger biological systems.

The number of observed structural conformers in supersonic jet experiments is typically much smaller compared to the number of stable species predicted by ab initio calculations with appreciable population at thermal equilibrium at room temperature. This can be understood since the collisional relaxation in the jet expansion promotes local minima to collapse to the lowest energy conformer if the dissociation energies of the complexes are small enough that repeated dissociation and recombination occur[28,35] or if the interconversion barriers between them are accessible.[43] Because of the large dissociation energies, we do not expect that the repeated dissociation and recombination of the complexes happen substantially under our current experimental condition. The observation of the six structural conformers of PO dimer suggests that the interconversion barriers between these conformers are relatively high that the collisional relaxations in the helium expansion do not interconvert these conformers readily. It is interesting to note that using heavier carrier gas such as neon seemed to enhance the interconversion between conformers. This point is manifested in our experiments by the fact that only one conformer, that is, *RR*2, was observed when using Ne as carrier gas instead of He. The intensities of the other five conformers were too weak to be observed, indicating substantial population transferring out of these local minima. This also explains the difficulty we encountered in the early stage of the spectral search when Ne was used. The observation may be understood by the fact that the collision energy of He with the complex is much smaller than that with Ne. Recently, Miller et al. reported a theoretical study of collision-induced conformational changes in glycine with He, Ne, and Ar.[44] They showed that, in addition to the energy of collision, attractive interactions between the heavier colliding atom such as Ne or Ar and the glycine molecule can catalyze conformer interconversion substantially. This may also be the case here, although detailed theoretical modeling is out of the scope of the current paper.

To establish the relative stability of the observed conformers, the intensities of the same rotational transitions of both the homo- and heterochiral species were measured under the same experimental condition with the same sample mixture using racemic PO.

The experimentally observed line intensities, scaled by the respective calculated dipole moment component values, give the following stability order: *RR*2 > *RR*4 ≈ *RS*4 > *RS*5 > *RR*5 > *RS*2. Comparing to a classic H-bond, one may expect the strength of the O_{epoxy}···H−C secondary H-bonds goes qualitatively with the negativity of the carbon atom involved. Since the carbon atoms of the CH_2 and CH groups are bonded directly to the more electron negative oxygen atom, we expect the electron negativity order for the carbon atom of each group to be CH_3 > CH_2 ≈ CH. For the homochiral diastereomers, the stability order *RR*2 (H3H2*R*-H3H1*R*) > *RR*4 (H3H2*R*-H2H1*R*) > *RR*5 (H3H1*R*-H2H1*R*) seems to correlate with the sum of the indexes which in turn tell us how many CH_3, CH_2, and CH types of secondary H-bonds there are in each conformer. However, the stability order of the heterochiral conformers is very different even though they utilize the same secondary

(40) Desiraju, G. R. In *The Weak Hydrogen Bond in Structural Chemistry and Biology*; Steiner, T., Ed.; Oxford University Press Inc: New York, 1999.
(41) Hobza, P.; Havlas, Z. *Chem. Rev.* **2000**, *100*, 4253−4264.
(42) Desiraju, G. R. *Chem. Commun.* **2005**, 2995−3001.
(43) Godfrey, P. D.; Rodgers, F. M.; Brown, R. D. *J. Am. Chem. Soc.* **1997**, *119*, 2232−2239. Godfred, P. D.; Brown, R. D. *J. Am. Chem. Soc.* **1998**, *120*, 10724−10732.
(44) Miller, T.F., III; Clary, D. C; Meijer, A. J. H. M. *J. Chem. Phys.* **2005**, *122*, 244323/1−13

Table 5. Experimental Results and Theoretical Dissociation Energies and Chiral Recognition Energies (in kJ/mol) of the Six Observed Conformers of PO Dimer

obs. conf.	exp. sign of ΔE_{chir}	MP2/6-311++ G**		MP2/aug-cc-p VDZ		MP2/aug-cc-p VTZ[a]	
		D_e + CP	ΔE_{chir}	D_e + CP	ΔE_{chir}	D_e + CP	ΔE_{chir}
*RR*2	<0	−14.97	−0.06	−18.09	−0.10	−19.45	0.24
*RS*2		−14.91		−17.99		−19.69	
*RR*4	∼0	−14.79	0.13	−17.65	0.10	−19.51	0.03
*RS*4		−14.92		−17.75		−19.54	
*RR*5	>0	−14.22	0.00	−17.12	−0.03	−18.90	−0.09
*RS*5		−14.22		−17.09		−18.81	

[a] Single-point energy calculation using MP2/aug-cc-pVTZ at the MP2/6-311++G(d,p) optimized geometries.

H-bonds as in the corresponding homochiral pairs. This is because such simple sum rule does not take into account other interactions such as steric hindrance effect, which will be discussed in relation to the chirodiastaltic energies in the next paragraph. The qualitative stability order observed is compared to the order predicted by the ab initio calculations in Table 5. As one can see, the stability trend observed is not well captured at either the MP2/6-311++G(d,p) or the MP2/aug-cc-pVDZ levels. Since the MP2/ 6-311++G(d,p) gives the best agreement with the experimental geometries, we performed single-point energy calculation with counterpoise correction at the MP2/aug-cc-pVTZ level with the MP2/6-311++G(d,p) optimized geometries. The accordingly obtained dissociation energies are also listed in Table 5 for comparison. However, they do not improve the degree of the agreement noticeably.

One interesting quantity here is the chirodiastaltic energy, ΔE_{chir}, the energy responsible for chiral recognition. It is defined as the energy difference between the homo- and heterochiral pair, that is, $\Delta E_{chir} = E_o(\text{homo}) - E_o(\text{hetero})$. A negative sign of ΔE_{chir} means that homochiral diastereomer is favored over the heterochiral one. According to the experimental observation, the largest negative chirodiastaltic energy among the six observed homo- and heterochiral diastereomers was found for the *RR*2 and *RS*2 pair where the *RR* conformer is favored. This is followed by a fairly small ΔE_{chir} for the *RR*4 and *RS*4 pair. Finally, a positive ΔE_{chir} was noted for the *RR*5 and *RS*5 pair where the heterochiral complex is preferred over the homochiral one. To aid the visualization, we use the HxHy*R*-Hx′Hy′*R*/*S* notation introduced earlier and fix the first subunit in the same position in each diastereomeric pair, as shown in Figure 1. One may correlate the chiral self-recognition observed here with the spatial orientation of the "discriminating" methyl group in the second subunit since this is the largest functional group attached to the stereogenic center. The distance between the two methyl C atoms in *RS*2 (H3H2*R*-H3H1*S*) is 3.984 Å as compared to 4.906 Å in *RR*2 (H3H2*R*-H3H1*R*). *RS*2 is therefore much less favored over *RR*2 because of the steric hindrance experienced by the methyl groups. Furthermore, since this discriminating methyl group is directly utilized in the secondary H-bonds, this pair has therefore the largest chiral discrimination energy. In the *RR*4 and *RS*4 (H3H2*R*-H2H1*R/S*) pair, chirality has little effect on their relative stability since the "discriminating" methyl group points away from the binding sites in both *RR*4 and *RS*4. In the last pair, *RR*5 (H3H1*R*-H2H1*R*) is less favored with a distance of 4.902 Å between the two methyl carbon atoms compared to 5.679 Å in *RS*5 (H3H1*R*-H2H1*S*). The overall discrimination effect, however, is smaller than in the *RR*2 and *RS*2 pair since the discriminating methyl group is further away from the binding sites and the two methyl groups are further apart than in the *RR*/*RS*2 pair. The ab initio ΔE_{chir} values for these six conformers are estimated using their corresponding counterpoise-corrected dissociation energies and are listed in Table 5 for comparison. It appears that even with the fairly large basis set such as aug-cc-pVTZ, it is still challenging for theoretical calculations to capture the subtle chiral recognition energy which can be unambiguously detected experimentally at the present time. The current experimental data for a relatively simple chiral diastereomer may serve as a benchmark system for future theoretical development in energy evaluation of this important class of molecular systems.

Conclusion

In summary, PO dimer was investigated with high-level ab initio methods and rotational spectroscopy. Three homochiral and the three corresponding heterochiral conformers of PO dimer were observed and assigned. The stability order and the sign of chiral recognition energies were determined experimentally, and the role of secondary H-bonds in chiral recognition was demonstrated. To the best of our knowledge, this is the first time that both homo- and the corresponding heterochiral dimers have been unambiguously identified via high resolution spectroscopy. The present results also show that the overall effect of several secondary H-bonds could be as significant as a single classic H-bond in stabilizing diastereoisomers and in determining spatial orientations of the binding partners. It will be of great interest to study other related chiral molecular complexes such as glycidol−PO complex and glycidol dimer, where one may expect larger chiral recognition effect because of the additional OH functional group.

Acknowledgment. This research was funded by the University of Alberta, the Natural Sciences and Engineering Research Council of Canada, the Canada Foundation for Innovation (New Opportunity), and an Alberta Ingenuity New Faculty Grant. Z S. thanks Alberta Ingenuity for a Studentship. N.B. thanks the German Academic Exchange Service (DAAD) and Alberta Ingenuity for Postdoctoral Fellowships.

Supporting Information Available: Completion of the reference 30. Summary of the calculation results with three different basis sets for the 12 structural conformers of PO dimer. Summary of all the measured transition frequencies of the six homo- and heterochiral conformers of PO dimer. Summary of the Cartesian coordinates of the 12 structural conformers of PO dimer. This material is available free of charge via the Internet at http://pubs.acs.org.

JA066128J